Gold Bull (2012) 45:153–160
DOI 10.1007/s13404-012-0059-4

ORIGINAL PAPER

Experimental and theoretical study on the synthesis of gold nanoparticles using ceftriaxone as a stabilizing reagent for and its catalysis for dopamine

Yuan-zhi Song · An-feng Zhu · Yang Song · Zhi-peng Cheng · Jian Xu · Jian-feng Zhou

Published online: 5 September 2012

Abstract Electrochemical synthesis of gold nanoparticles on the surface of glassy carbon electrode and preparation of GNPs in aqueous solution using ceftriaxone as an innocuous stabilizing reagent were proposed. The gold nanoparticles were characterized by scanning electron microscopy, transmission electron microscopy, infrared spectrometry, UV spectrophotometry, powder X-ray diffraction, and cyclic voltammetry. The catalysis of gold nanoparticles on the glassy carbon electrode for dopamine was demonstrated. The results indicate that the modified electrode has an excellent repeatability and reproducibility. The relationship between the molecular structure and the dispersion of GNPs on the surface of GCE as well as the catalysis of GNPs for dopamine was discussed.

Keywords Gold nanoparticles · Synthesis · Ceftriaxone · Stabilizing reagent

Introduction

Gold nanoparticles (GNPs) have been widely used in the fields of physics, chemistry, biology, medicine, and material science [1]. To maximize the efficiency of GNPs in their applications, well-controlled particle size, efficient particle dispersion, and excellent reproducibility are necessary. The strategies for immobilization of GNPs layers onto the surfaces include electrostatic links and covalent bonding. The surface of functional groups (COOH, OH, SH, and NH_2) are suitable substrate for the deposition of GNPs [2–5]. The reduction of $HAuCl_4$ is the most used methods for the preparation of GNPs in aqueous solution; reductants such as ascorbic acid [6], citrate [7–9], and borohydride [10, 11] have been used in this reaction. Electrochemical deposition of metal nanoparticles has been found a better alternative because of their flexibility in controlling the size and coverage of the metal nanoparticles [12, 13].

However, it is difficult to control the size of GNPs in the aqueous solution because the size of the GNPs in aqueous solution is commonly controlled by changing the reaction parameters such as molar ratio of the reductant, gold precursor, pH, temperature, the stabilizing reagent, and the prepared process is time consuming. The stabilizing reagent of GNPs is most important factor; the size and dispersion are controlled mainly by the molecule of stabilizing reagent. Therefore, the relationship between the size and dispersion and the molecular is an interesting topic.

Cefoperazone, formerly known as cefoperazone sodium, is a semisynthetic, broad-spectrum cephalosporin antibiotic. Chemically, cefoperazone sodium is sodium of (6*R*,7*R*)-7-[(*R*)-2-(4-ethyl-2,3-dioxo-1-piperazinecarboxamido)-2-(*p*-hydroxyphenyl)-acetamido-3-[[(1-methyl-1*H*-tetrazol-5-yl)thio]methyl]-8-oxo-5-thia-1-azabicyclo[4.2.0]oct-2-ene-2-carboxylate. Its molecular formula is $C_{25}H_{26}N_9NaO_8S_2$ with a molecular weight of 667.65 [14]. The goals of this paper demonstrate ceftriaxone's versatile role in stabilizing GNPs prepared by electrochemical deposition and wet-chemistry reduction.

Our previous works have indicated that density-functional theory is a powerful method for predicting the geometry and harmonic vibration of organic compounds [15–19]. Therefore, the DFT-B3LYP/6-31G (d, p) was carried out to study the molecular structure of ceftriaxone.

Y.-z. Song (✉) · A.-f. Zhu · Z.-p. Cheng · J.-f. Zhou
Jiangsu Province Key Laboratory for Chemistry of Low-Dimensional Materials, School of Chemistry and Chemical Engineering, Huaiyin Normal University, Huai An 223300, People's Republic of China
e-mail: singyuanzhi@126.com

Y. Song (✉) · J. Xu
College of Materials Science and Engineering, Beijing University of Chemical Technology, Peking 100029, People's Republic of China
e-mail: songyang@mail.buct.edu.cn

In present work, ceftriaxone as an innocuous stabilizing reagent was used for electrochemical synthesis of GNPs on the surface of glassy carbon electrode (GCE) and preparation for GNPs in aqueous solution for a stable sensor, DFT-B3LYP/6-31G (d, p) was carried out to study the molecular structure and the properties of ceftriaxone. The catalysis of GNPs for dopamine at ceftriaxone@GNP/GCE and GNP/GCE was demonstrated. The relationships between the molecular structure of ceftriaxone and the dispersion of GNPs on the surface of GCE as well as the catalysis of GNPs for dopamine were discussed.

Experimental

Materials

All reagents used herein were of analytical grade. Doubly distilled water was used throughout; 0.1 M phosphate-buffered solution (PBS) was prepared by dissolving 0.1 mol NaCl and 0.1 mol Na_2HPO_4 in double-distilled water of 1,000 mL and adjusted desired pH values with 6 M HCl or 1 M NaOH.

Preparation of GNPs

The GNPs were deposited at a voltage of −0.2 V for 30 s on the surface of GCE that was immersed in the mixture of $HAuCl_4$ (2.0 mg mL^{-1}), H_2SO_4 (0.5 M), and ceftriaxone sodium (0.4 mg mL^{-1}), and then washed in doubly distilled water. In the typical synthetic process of GNPs in aqueous solution, 0.150 g of $NaBH_4$ were dissolved into the mixture of 2.0 mg mL^{-1} $HAuCl_4$, 0.5 mol L^{-1} H_2SO_4, and 0.4 mg mL^{-1} ceftriaxone sodium. The solution was stirred with a magnetic stirrer for 10 min to ensure that the $NaBH_4$ completely dissolved; the black GNPs were soon produced, and followed by centrifugal separation, washing with absolute alcohol and drying in vacuum at 20 °C for 6 h.

Characterization

For all electrochemical experiments, a CHI660B Electrochemical Analyzer (CHI, USA) was employed. The GNP-modified GCE was used as working electrode, a platinum wire served as the counter electrode, and a saturated calomel electrode was used as the reference electrode. The GNPs were characterized by scanning electron microscope (SEM; S-4800, HITACHI, Japan), transmission electron microscope (TEM, JEM 2100, JEOL, Japan), UV spectrophotometer (UV-1750, Shimadzu, Japan). Powder X-ray diffraction (XRD) spectra were recorded on a Switzerland ARL/X'TRA X-ray diffractometer rotating anode with Cu-Kα radiation source (λ=1.54056 Å). IR spectra were measured by a NICOLET NEXUS470 spectrometer in the frequency range 4,000–400 cm^{-1}.

Calculation

The calculations of ceftriaxone were performed with the Gaussian03 package [20]. The molecule in the vacuum was fully optimized using DFT-B3LYP with the 6–31G (d, p) basis sets.

Results and discussion

SEM and TEM images of GNPs

SEM images confirm the formation of a layer of GNPs on the GCE surface, several GNPs on the surface of GCE in presence of ceftriaxone were observed in Fig. 1a and b, and those on the surface of GCE in absence of ceftriaxone are shown in Fig. 1c, indicating that the well-dispersed GNPs on the surface of GCE in the presence of ceftriaxone were obtained. The size of GNPs deposited at −0.2 V for 30 s (Fig. 1a) are larger than those obtained at same potential for 10 s (Fig. 1b), indicating that the size of GNPs on the surface of GCE were controlled by the reduction time of $HAuCl_4$. The TEM images of GNPs obtained from aqueous solution were shown in Fig. 1b, the size of GNPs is about 25–100 nm. The GNPs on the GCE surface is similar to those in aqueous due to the reduction of $HAuCl_4$. From the molecular structure of ceftriaxone it can be seen that the gold atoms of surface of GNPs adsorb the negative ions (ceftriaxone) with the polar groups such as carbonyl, carboxyl, and amidocyanogen. Therefore, the GNPs on the surface of GCE are well dispersed.

XRD of GNPs

The powder XRD pattern of the GNPs from aqueous solution is shown in Fig. 2. The major diffraction peaks can be indexed as the gold face-centered cubic (fcc) phase based on the data of the JCPDS file (JCPDS no. 04-0784) [21]. The diffraction peaks of GNPs appeared at 38.7°, 44.6°, 64.4°, and 78.7°, which can be assigned to (111), (200), (220), and (311) crystalline plane diffraction peaks of gold, respectively. The diffraction peaks at 16.0° and 27.9° may be assigned to the ceftriaxone. On the nanometer scale metals (most of them are fcc) tend to nucleate and grow into twinned and multiple twinned particles with their surfaces bounded by the lowest-energy (111) facets [22]. Other morphologies with less stable facets have only been kinetically achieved by adding chemical capping reagents to the synthetic systems [23–26].

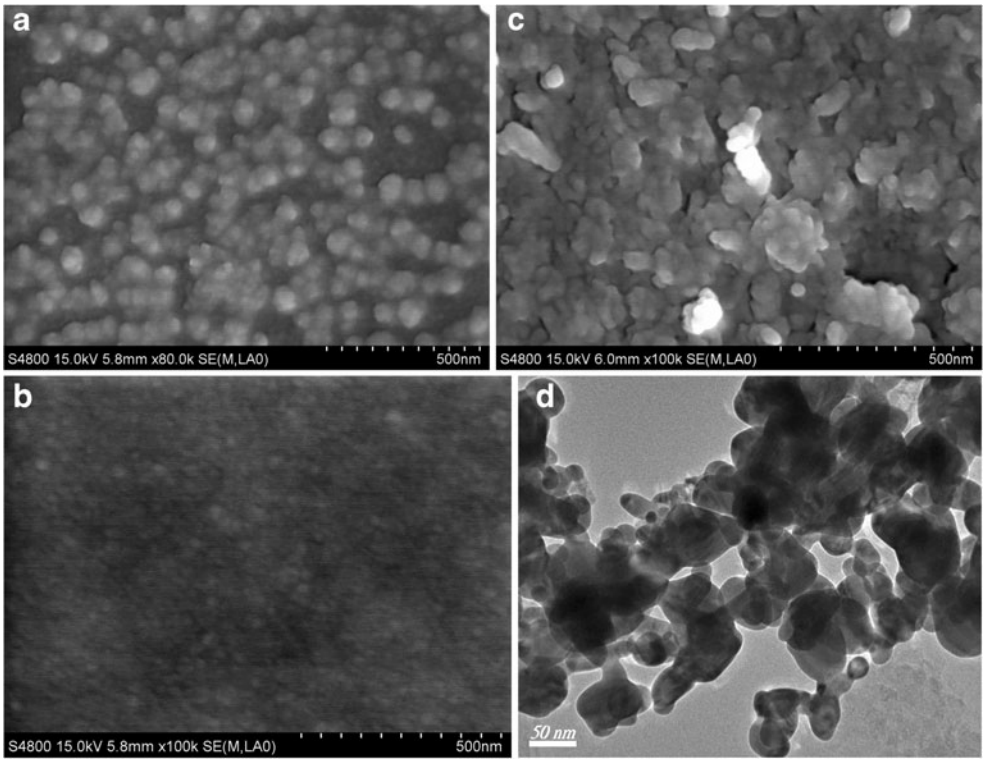

Fig. 1 SEM images of GNPs on the surface of GCE deposited at −0.2 V for 30 (**a**), 10 (**b**) in presence of ceftriaxone, and 30 s in absence of ceftriaxone (**c**), and TEM images of GNPs prepared by sodium borohydride reduction (**d**)

IR spectra of GNPs

The IR spectra of GNPs obtained from GCE and ceftriaxone are shown in Fig. 3. From the IR spectra of ceftriaxone, the bands at 3,436 and 3,244 cm^{-1} could be assigned to the stretching vibrations of NH and OH, the bands of stretching vibrations of CH were found at 2,930 and 2,816 cm^{-1}, the band of stretching vibrations of C=O appeared at 1,743, 1,647, and 1,613 cm^{-1}, and the peaks at 1,535 and 1,499 cm^{-1} were associated with the torsional vibrations of aromatic ring. The bands at 1,395 and 1,359 cm^{-1} could be assigned to stretching vibrations of CN, and band of breath vibration of aromatic ring was observed at 1,037 cm^{-1} [27]. However, the IR spectra of GNPs obtained from GCE, the bands of stretching vibrations of NH and OH were found at 3,402 and 3,130 cm^{-1}, the band at 1,621 cm^{-1} could be assigned to the stretching vibrations of C=O, the bands of stretching vibrations of CN and the breath vibration of aromatic ring were found at 1,403 and 1,081 cm^{-1}, respectively, indicating ceftriaxone was assembled on the surface of GNPs.

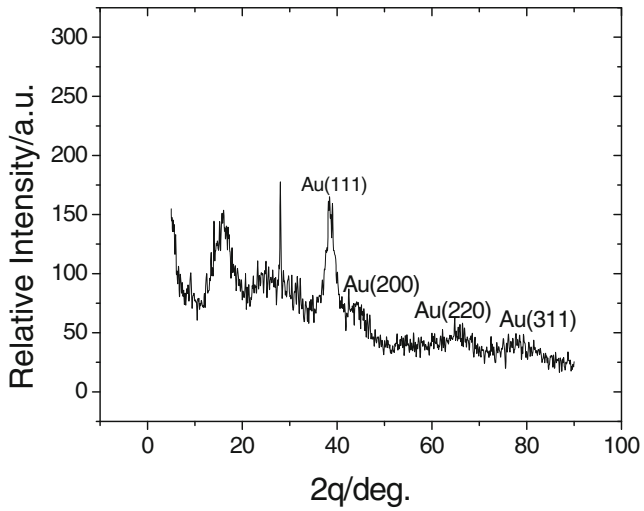

Fig. 2 XRD pattern of GNPs obtained from aqueous solution

UV spectra of GNPs

Figure 4 shows the UV absorption spectrum of the GNPs obtained from aqueous solution. A broad band centered at ca. 557 nm appears, characteristic of surface plasmon absorption on the GNPs.

Cyclic voltammograms of GNPs

The cyclic voltammograms (CVs) of GNPs on the surface of GCE in 0.1 M PBS of pH 7.3 are shown in Fig. 5. The oxidation peak of ceftriaxone@GNPs was found at 1.118 V, and the reduction peak was observed at 0.459 V. To remove ceftriaxone on the surface of GNPs, the ceftriaxone@GNPs-modified GCE was rinsed with a magnetic stirrer in 5 mol L^{-1} H_2SO_4 aqueous solution and doubly distilled

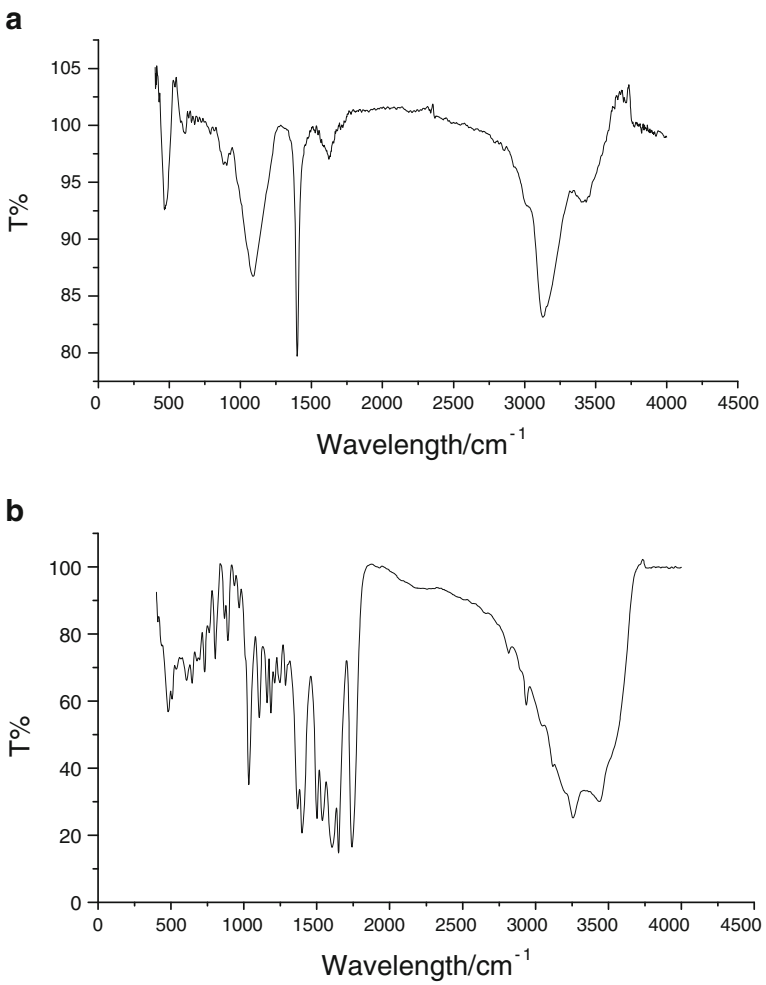

Fig. 3 IR spectra of GNPs obtained from the surface of GCE (**a**) and ceftriaxone (**b**)

water for 10 min, sequentially. The peak potential of the rinsed GNPs shifted to positive direction, and the reduction current increases, indicating the ceftriaxone on the surface of GNPs was removed. The CVs of ceftriaxone at GCE are shown in Fig. 5 (inset), an oxidation peak was observed at 1.153 V, and a reduction peak at 0.900 V was observed, which was assigned to the sulfur atoms in ceftriaxone,

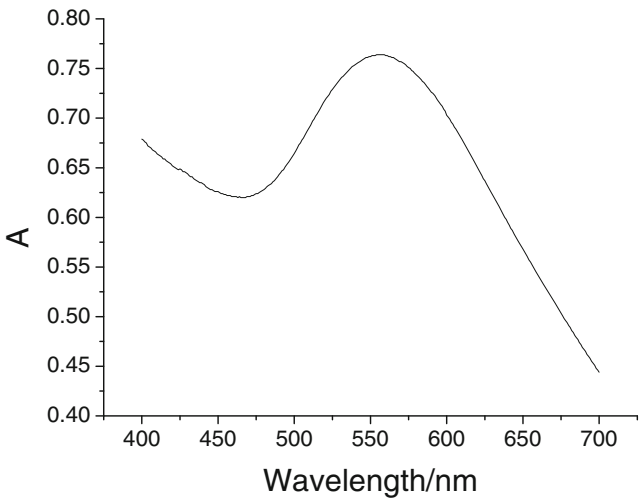

Fig. 4 UV spectra of GNPs in absolute alcohol

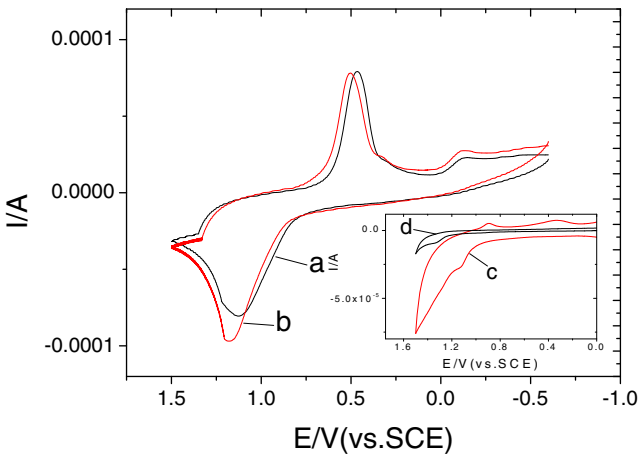

Fig. 5 CVs of the ceftriaxone@GNPs (*a*) and rinsed GNP/GCE (*b*). Supporting electrolyte: 0.1 mol L^{-1} PBS of pH 7.3. *Inset* CVs of 0.4 mg/mL ceftriaxone sodium at GCE (*c*) and bare GCE (*d*), supporting electrolyte, 0.5 mol L^{-1} H_2SO_4

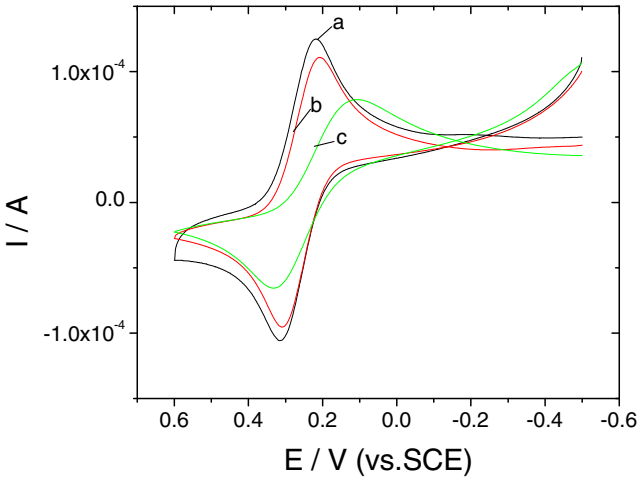

Fig. 6 CVs of 5 mM $K_4[Fe(CN)_6]$ at ceftriaxone@GNP/GCE (*a*), rinsed GNP/GCE (*b*), and bare GCE (*c*). Supporting electrolyte, 0.1 mol L^{-1} KCl

indicating that ceftriaxone is stable under electrochemical synthesis of ceftriaxone@GNPs at −0.2 V.

CVs of GNP-modified GCE in the $K_3Fe(CN)_6$–$K_4Fe(CN)_6$ system

The CVs of GNP modified GCE in the $K_3Fe(CN)_6$–$K_4Fe(CN)_6$ system were shown in Fig. 6. The real active surface

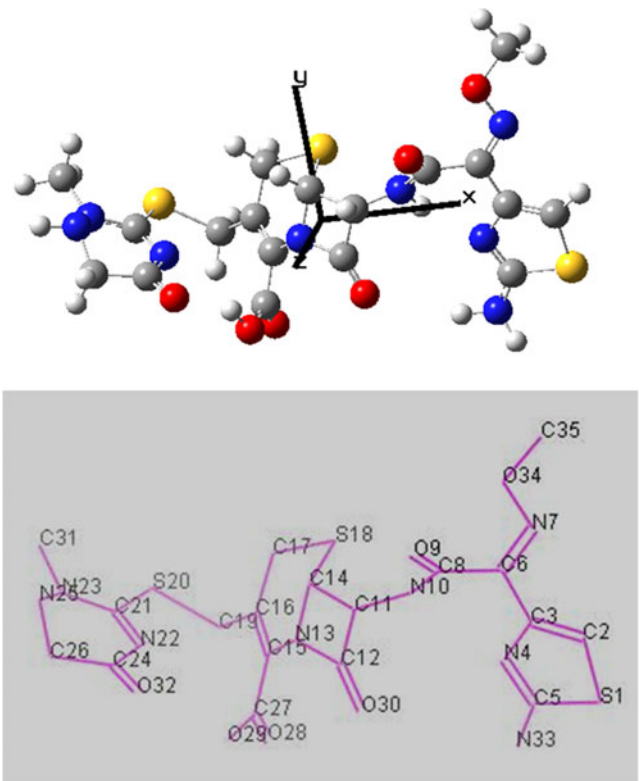

Fig. 7 Geometry and numbering atoms of ceftriaxone

Table 1 Mülliken charge of atoms in ceftriaxone

Atom	Mülliken charge
S_1	0.225548
N_4	−0.52594
N_7	−0.20545
O_9	−0.48835
N_{10}	−0.21175
N_{13}	−0.50661
S_{18}	0.141123
S_{20}	0.134278
N_{22}	−0.51138
N_{23}	−0.32606
N_{25}	−0.09105
O_{28}	−0.45712
O_{29}	−0.14326
O_{30}	−0.46103

area will be estimated. In a reversible process, the following Randles-Sevcik formula [28] at 298 K has been used:

$$i_p = 2.69 \times 10^5 n^{3/2} A\, C_o D_o{}^{1/2} v^{1/2}.$$

Where i_p is the peak current (amperes), n the number of electrons, A the electrode area (in square centimeters), C the concentration (in moles per cubic centimeter), D the diffusion coefficient (in square centimeters per second), and v the scan rate (in volts per second).

From the slope of the plot of oxidation current (i_p) versus $\upsilon^{1/2}$, the electrode surface area of the ceftriaxone@GNP/GCE, GNP/GCE, and the bare GCE is 0.115, 0.104, and 0.071 cm^2, respectively, indicating that the microscopic area of the GNP/GCE increased significantly and was about 1.46 times larger than the microscopic area of the bare GCE.

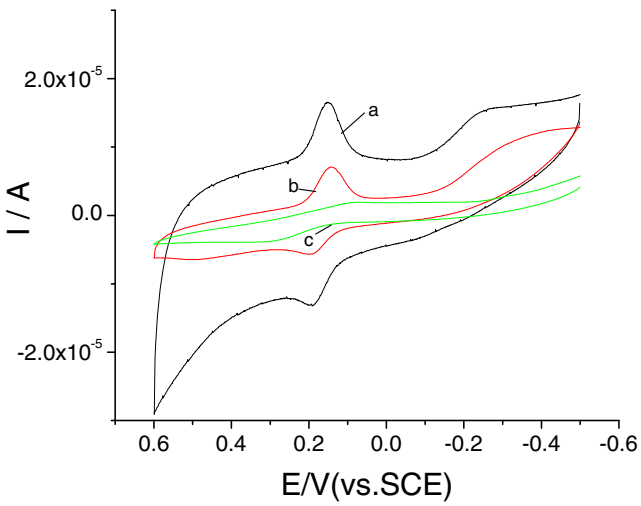

Fig.8 CVs of 80.0 mg L^{-1} dopamine at ceftriaxone@GNP/GCE (*a*), the rinsed GNP/GCE (*b*), and bare GCE (*c*). *Scan rate* 100.0 mV s^{-1}. Supporting electrolyte: 0.1 mol L^{-1} PBS of pH 7.3

Table 2 Peak and current of dopamine

Electrode	Oxidation peak (V)	Oxidation current (μA), unit current (μA cm^{-2}/mg L^{-1})	Reduction peak (V)	Reduction current (μA), unit current (μA cm^{-2}/mg L^{-1})
Bare GCE	0.276	1.14, 1.61	0.090	0.88, 1.24
GNP/GCE	0.194	3.64, 3.50	0.140	5.21, 5.01
Ceftriaxone@GNP/GCE	0.191	6.80, 5.91	0.151	7.11, 6.18
GNP/DWCNT/GCE[12]	0.247	108.5, 14.37	0.148	69.39, 9.19

Optimized geometry and molecular properties of ceftriaxone

The molecular property is controlled by the structure. Ceftriaxone is an organic acid, the degree of ionization for ceftriaxone are controlled by sulfuric acid, thus the optimized geometry of protonated ceftriaxone at DFT-B3LYP/6–31G (d, p) level is shown in Fig. 7. It can be seen in Fig. 7 that the hydrophilic carbonyl and carboxyl locate at a side of ceftriaxone, while hydrophobic methylene and methyl appear at another side. The Mülliken charges with hydrogen summed into heavy atoms for ceftriaxone are listed in Table 1, in Table 1 the negative atoms are oxygen and nitrogen. The total dipole moment (vector X=−7.0061, Y=3.9098, Z=−1.7552) of ceftriaxone is 8.2130 Debye, indicating that the negative electron cloud in ceftriaxone shifted to X direction. Therefore, the coordination bonds form between the gold atoms of surface of GNPs and the oxygen (O_{28}, O_{30}, and O_{34}) and nitrogen (N_4) in ceftriaxone, the hydrophobic ceftriaxone@GNP on the surface of GCE is well dispersed due to the absorbed ceftriaxone on the surface of the GNPs.

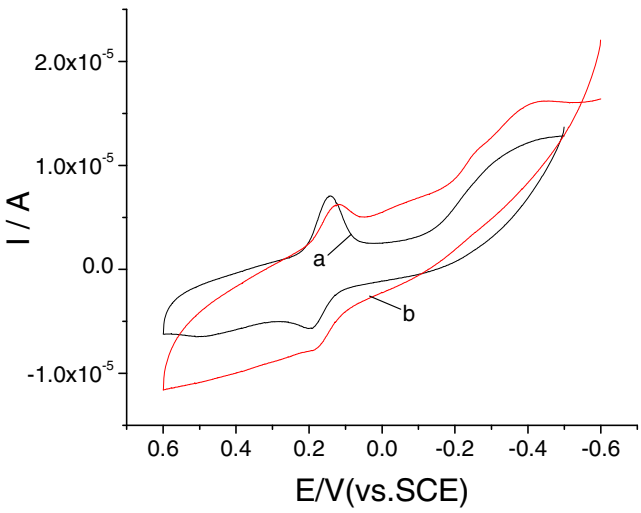

Fig. 9 CVs of 10.0 mg L^{-1} dopamine at GNP/GCE prepared by electrochemical deposition (*a*) and absorption method (*b*). Scan rate, 100.0 mV s^{-1}. Supporting electrolyte, 0.1 mol L^{-1} PBS of pH 7.3

Electrochemical catalysis of GNP

Dopamine is important in the regulation of sodium balance and blood pressure via renal mechanisms [29, 30]. The affinity of dopamine for its receptors is in the nanomolar range; higher concentrations occupy other G-protein-coupled receptor [29, 30]. Circulating dopamine concentrations (picomolar range) are not sufficiently high to activate dopamine receptors, but high nanomolar concentrations can be attained in dopamine-producing tissues (e.g., renal proximal tubule, jejunum). The concentration of dopamine is controlled by not only the taking drugs but also the human emotion. Therefore, the determination of dopamine in blood is important.

The CVs of dopamine at bare GCE, ceftriaxone@GNP/GCE, and rinsed GNP/GCE are shown in Fig. 8, respectively. The peak potentials, currents, and unit currents (the currents per square centimeter of electrode area for 1 mg L^{-1} dopamine, μA/cm^{-2}/mg L^{-1}) of dopamine at bare GCE, ceftriaxone@GNP/GCE, and rinsed GNP/GCE are summarized in Table 2. For comparison with the gold nanoparticle/double-walled carbon nanotube-modified glassy carbon electrode (GNP/DWCNT/GCE), the currents and unit currents for 50 mg L^{-1} dopamine hydrochloride at GNP/DWCNT/GCE are also shown in Table 2 [12]. The sensitivity of GNP/GCE for dopamine is lower than that GNP/DWCNT/GCE. However, when stirring the solution for renewing the modified electrode, the GNP/DWCNT on the surface of GCE removed easily due to adsorption of DWCNTs. Therefore, the GNP/GCE is more stable than GNP/DWCNT/GCE. It can be seen in Table 2 that the oxidation potential for dopamine at the rinsed GNP/GCE and ceftriaxone@GNP/GCE are less than that of dopamine at bare GCE, and their currents are higher than that of dopamine at bare GCE. However, the currents for dopamine at the ceftriaxone@GNP/GCE are higher than that of dopamine at the rinsed GNP/GCE, indicating that ceftriaxone catalyzes the redox of dopamine due to the formation of hydrogen bond between ceftriaxone and dopamine.

CVs of 10.0 mg L^{-1} dopamine at GNP/GCE prepared by electrochemistry deposition and absorption method are shown in Fig. 9, compared with the oxidation currents (2.24 μA) at 0.185 V and reduction currents (2.12 μA) at

0.122 V for dopamine at GNP/GCE prepared by absorption method, both oxidation currents (3.60 μA) at 0.193 V and reduction currents (5.20 μA) at 0.142 V for dopamine at GNP/GCE prepared by electrochemical deposition increase, indicating that the GNPs on the surface of GCE prepared by electrochemical deposition catalyze dopamine well, the results may be ascribe to the well dispersion of GNPs on the surface of GCE prepared by electrochemical deposition.

On using the rinsed GNPs/GCE daily and storing under ambient conditions over a period of 2 months, and after stirring at 700 rpm/min with a magnetic stirring apparatus for 2 h, the electrode retained 96.5 % of its initial peak current response with relative standard deviation (RSD) of 2.3 % (n= 25) for a dopamine concentration of 80.00 mg L^{-1}, which shows long-term stability of the film modifier on the surface of GCE. The results indicate that the rinsed GNPs/GCE has an excellent repeatability and reproducibility. However, the GNPs obtained from aqueous solution dropped on the surface of GCE as the adsorption method, followed by storage at 14 °C for 24 h, after stirring at 700 rpm/min with a magnetic stirring apparatus for 2 h the modified GCE retained 86.5 % of its initial peak current response with RSD of 4.3 % (n=25) for a dopamine concentration of 80.00 mg L^{-1}.

Conclusions

The gold nanoparticles on the surface of GCE and in aqueous solution using ceftriaxone as a stabilizing reagent were prepared in this paper, and the catalysis of ceftriaxone@GNPs and GNPs for dopamine was demonstrated. The sensitivity of GNP/GCE for dopamine is lower than that GNP/DWCNT/GCE. However, the GNP/GCE is more stable than GNP/DWCNT/GCE, and the electrochemical synthesis of ceftriaxone@GNPs on the surface of glassy carbon is simple, cheap, and rapid. The relationships between the molecular structure of ceftriaxone and the dispersion of GNPs on the surface of GCE as well as the catalysis of GNPs for dopamine were discussed, and the rinsed GNPs/GCE has an excellent repeatability and reproducibility.

Acknowledgments The authors gratefully acknowledge the financial support of the National Science Foundation of China (grant nos. 51175245 and 51106061), the Science Foundation of Education of Jiangsu Province of China (grant no. JH10-48), the Open Science Foundation for Jiangsu Province Key Laboratory for Chemistry of Low-Dimensional Materials (grant no. JSKC11091), and the Science Foundation for Huaiyin Normal University (grant no. 11HSGJBZ13).

References

1. Rashid MH, Bhattacharjee RR, Kotal A, Mandal TK (2006) Synthesis of spongy gold nanocrystals with pronounced catalytic activities. Langmuir 22:7141–7143
2. Mena ML, Yánz-Sedeño P, Pingarrõn JM (2006) A comparison of different strategies for the construction of amperometric enzyme biosensors using gold nanoparticle-modified electrodes. Anal Biochem 336:20–27
3. He P, Urban MW (2005) Phospholipid-stabilized Au− nanoparticles. Biomacromolecules 6:1224–1225
4. Qi ZM, Zhou HS, Matsuda NK, Honma I, Shimada K, Takatsu A, Kato K (2004) Characterization of gold nanoparticles synthesized using sucrose by seeding formation in the solid phase and seeding growth in aqueous solution. J Phys Chem B 108:7006–7011
5. Zubarev ER, Xu J, Sayyad A, Gibson JD (2006) Amphiphilic gold nanoparticles with V-shaped arms. J Am Chem Soc 128:4958–4959
6. Luty-Błocho M, Fitzner K, Hessel V, Löb P, Maskos M, Metzke D, Pacławski K, Wojnicki M (2011) Synthesis of gold nanoparticles in an interdigital micromixer using ascorbic acid and sodium borohydride as reducers. Chem Eng J 171:279–290
7. Koutsoulis NP, Giokas DL, Vlessidis AG, Tsogas GZ (2010) Alkaline earth metal effect on the size and color transition of citrate-capped gold nanoparticles and analytical implications in periodate-luminol chemiluminescence. Anal Chim Acta 669:45–52
8. Balasubramanian SK, Yang L, Yung L-Y L, Ong C-N, Ong W-Y, Yu LE (2010) Characterization, purification, and stability of gold nanoparticles. Biomaterials 31:9023–9030
9. Mikhlin Y, Karacharov A, Likhatski M, Podlipskaya T, Zubavichus Y, Veligzhanin A, Zaikovski V (2010) Submicrometer intermediates in the citrate synthesis of gold nanoparticles: new insights into the nucleation and crystal growth mechanisms. J Colloid Interf Sci 362:330–336
10. Seoudi AA, Fouda DA (2010) Synthesis, characterization and vibrational spectroscopic studies of different particle size of gold nanoparticle capped with polyvinylpyrrolidone. Physica B 405:906–911
11. He P, Zhu X (2007) Phospholipid-assisted synthesis of size-controlled goldnanoparticles. Mater Res Bull 42:1310–1315
12. Song YZ, Song Y, Zhong H (2011) L-cysteine-nano-gold modified glassy carbon electrode and its application for determination of dopamine hydrochloride. Gold Bull 44:107–111
13. Song Y, Song YZ, Zhu AF, Zhong H (2011) Indian J Chem A 50A:1006–1009
14. Arguedas A, Loaiza C, Perez A, Gutierrez A, Herrera ML, Rothermel CD (2003) A pilot study of single-dose azithromycin versus three-day azithromycin or single-dose ceftriaxone for uncomplicated acute otitis media in children. Curr Ther Res 64:16–29
15. Song YZ, Zhou JF, Song Y, Wei YG, Wang H (2005) Density-functional theory studies on standard electrode potentials of half reaction for L-adrenaline and adrenalinequinone. Bioor Med Chem Lett 15:4671–4680
16. Song YZ, Ruan M, Ye Y, Li YY, Xie W, Shen J, Shen AG (2008) Experimental and density functional theory and ab initio Hartree–Fock study on the vibrational spectra of 2-(4-fluorobenzylideneamino)-3-(4-hydroxyphenyl) propionic acid. Spectrochim Acta Part A 69:682–687
17. Song YZ (2007) Theoretical study on the electrochemical behavior of norepinephrine at Nafion multi-walled carbon nanotubes modified pyrolytic graphite electrode. Spectrochim Acta Part A 67:1169–1177
18. Song YZ, Zhang LL, Zhong H, Shi DQ, Xie JM, Zhao GQ (2008) Theoretical study on the geometry and vibration of 1-{6-(4-chlorophenyl)-1-[(6-chloropyridin-3-yl)methyl]-2-[(6-chloropyridin-3-

yl)methylsulfanyl]-4-methyl-1,6-dihydropyrimidin-5-yl}ethanone. Spectrochim Acta Part A 70:943–952
19. Shi DQ, Zhu XF, Song YZ (2008) Synthesis, crystal structure, insecticidal activity and DFT study on the geometry and vibration of *O*-(*E*)-1-{1-[(6-chloropyridin-3-yl) methyl]-5-methyl-1*H*-1,2,3-triazol-4-yl}ethyleneamino-*O*-ethyl-*O*-phenylphosphorothioate. Spectrochim Acta Part A 71:1011
20. Frisch MJ, Trucks GW, Schlegel HB, Scuseria GE, Robb MA, Cheeseman JR, Montgomery JA, Vreven JT, Kudin KN, Burant JC, Millam JM, Iyengar SS, Tomasi J, Barone V, Mennucci B, Cossi M, Scalmani G, Rega N, Petersson GA, Nakatsuji H, Hada M, Ehara M, Toyota K, Fukuda R, Hasegawa J, Ishida M, Nakajima T, Honda Y, Kitao O, Nakai H, Klene M, Li X, Knox JE, Hratchian HP, Cross JB, Bakken V, Adamo C, Jaramillo J, Omperts R, Stratmann RE, Yazyev O, Austin AJ, Cammi R, Pomelli C, Ochterski JW, Ayala PY, Morokuma K, Voth GA, Salvador P, Dannenberg JJ, Zakrzewski VG, Dapprich S, Daniels AD, Strain MC, Farkas O, Malick DK, Rabuck AD, Raghavachari K, Foresman JB, Ortiz JV, Cui Q, Baboul AG, Clifford S, Cioslowski J, Stefanov BB, Liu G, Liashenko A, Piskorz P, Komaromi I, Martin RL, Fox DJ, Keith T, Al-Laham MA, Peng CY, Nanayakkara A, Challacombe Gill MPM, Johnson B, Chen W, Wong MW, Gonzalez C, Pople JA (2004) Gaussian Inc, Wallingford
21. Joint Committee on Powder Diffraction Standards (1991) Diffraction Data File: JCPDS International Center for Diffraction Data. Swarthmore PA
22. Allpress JG, Sanders JV (1967) The structure and orientation of crystals in deposits of metals on mica. Surf Sci 7:1–25
23. Bradley JS, Tesche B, Busser W, Maase M, Reetz MT (2000) Surface spectroscopic study of the stabilization mechanism for shape-selectively synthesized nanostructured transition metal colloids. J Am Chem Soc 122:4631–4636
24. Puntes VF, Krishnan KM, Alivisatos AP (2001) Colloidal nanocrystal shape and size control: the case of cobalt. Science 291:2115–2117
25. Kirkland AI, Jefferson DA, Duff DG, Edwards PP, Gameson I, Johnson BFG, Smith D (1993) Structural studies of trigonal lamellar particles of gold and silver. Proc R Soc Lond Ser A 440:589–609
26. Ahmadi TS, Wang ZL, Green TC, Henglein A, El-Sayed MA (1996) Shape-controlled synthesis of colloidal platinum nanoparticles. Science 272:1924–1925
27. Cordente N, Respaud M, Senocq F, Casanove M-J, Amiens C, Chaudret B (2001) Synthesis and magnetic properties of nickel nanorods. Nano Lett 1:565–568
28. Kissinger PT, Heineman WR (1984) Laboratory techniques in electroanalytical chemistry Chapter 3. Marcel Dekker, New York
29. Zeng C, Armando I, Luo Y, Eisner GM, Felder RA, Jose PA (2008) Dysregulation of dopamine-dependent mechanisms as a determinant of hypertension: studies in dopamine receptor knockout mice. Am J Physiol Heart Circ Physiol 294:H551–H569
30. Hussain T, Lokhandwala MF (2003) Renal dopamine receptors and hypertension. Exp Biol Med (Maywood) 228:134–142